Regular article

PHYSICAL CHEMISTRY RESEARCH
Published by the
Iranian Chemical Society
www.physchemres.org
info@physchemres.org

***Phys. Chem. Res.**, Vol. 1, No. 1, 41-51, June 2013.*

High-Level Quantum Chemical Calculations of Ozone-Water Complexes

H. Roohi[a,*] and E. Ahmadepour[b]

[a]*Department of Chemistry, Faculty of Science, University of Guilan, Department of Chemistry, Rasht, Iran*

[b]*Islamic Azad University of Persian Branch, Bandar Abbas, Iran*

(Received 27 October 2012, Accepted 22 December 2012)

The structural and energetic characteristics of O_3-H_2O complexes have been investigated by means of B3LYP, MP2, MP4(SDTQ), CCSD(T) and QCISD(T) methods in conjunction with AUG-cc-pVDZ and AUG-cc-pVTZ basis sets. Six conformers were found for the O_3-H_2O complex. Two different intermolecular interactions were expected to participate in the formation of complexes, namely conventional O···H hydrogen bonding and O···O interaction. The most stable structure is non-hydrogen bonded one with double O···O interactions. The binding energies of the most stable complex, corrected with BSSE and ZPE, range from -5.99 to -12.20 kJ mol^{-1} at CCSD(T)/AUG-cc-pVTZ, QCISD(T)/AUG-cc-pVTZ and MP4(SDTQ)/AUG-cc-pVTZ high levels of theory. The equilibrium distance between centers of monomers (O_3···OH_2) in the most stable complex at the CCSD(T)/AUG-cc-pVDZ and CCSD(T)/AUG-cc-pVTZ levels is 2.9451 and 2.9448 Å, respectively, in good agreement with the experimental value of 2.957 Å. The AIM calculations predict that the O···O and O···H interactions in O_3-H_2O complexes are electrostatic in nature.

Keywords: O_3-H_2O complexes, Quantum chemical calculations, Non-hydrogen bonded interaction

INTRODUCTION

Non-covalent interactions play an important role in determining of the structure of different systems in many areas such as atmospheric chemistry. The chemistry of ozone is important in explaining of the depletion of the ozone layer by a series of reactions between ozone and other atmospheric compounds. Thus, reaction of ozone with another species is one of the best investigated chemical reactions reported in many research papers in the recent years [1-19]. The hydroxyl radical OH in atmosphere is generated by following reactions.

$$O_3 + h\nu \rightarrow O(^1D) + O_2$$

$$O(^1D) + H_2O \rightarrow 2OH$$

The OH radical is known as the primary oxidant in the daytime chemistry [20,21]. Also, it has been predicted [22,23] that the O_3-H_2O complex is another source of OH radical in the troposphere according to the reaction:

$$O_3\text{-}H_2O + h\nu \rightarrow 2OH + O_2$$

*Corresponding author. E-mail: hroohi@guilan.ac.ir

The microwave spectrum of the O_3-H_2O complex in gas phase has been observed with a pulsed-beam Fabry-Perot cavity Fourier-transform microwave spectrometer [7]. The A_1 spectra of O_3-H_2O, O_3-$H_2{}^{18}O$ and O_3-D_2O as well as the O_3-HDO spectrum were fitted to a Watson asymmetric top Hamiltonian, giving A = 11960.58, B = 4174.036 and C = 3265.173(8) MHz for O_3-H_2O.

The structure of the O_3-H_2O complex were recently studied at B3LYP/6-311++G(d,p) [4], CCSD/6-311++G(d,p) [6] and QCISD/6-311++G(d,p) levels [2,6] by Tachikawa and Abe. They reported three structures as stable forms of O_3-H_2O complex. In their first publication they deduced that the most stable structure is a dipole orientation form with all atoms of H_2O and the central oxygen atom of the O_3 located in the molecular C_s plane [2]. The second and third structures were *cis* and *trans* forms where all atoms lie in the C_s molecular plane. In the last article, they suggested that the most stable structure of the O_3-H_2O complex is the eclipsed form where the oxygen atom of H_2O and the central oxygen atom of O_3 located in the molecular C_s plane.

Recently, Tsuge *et al.* [24] have applied matrix isolation infrared spectroscopy together with *ab initio* calculations at the CCSD(T), QCISD and MP4(SDQ) levels to study the ozone-water complex. They have demonstrated the existence

of only one stable conformer (double-decker). This conformer belongs to the C_s symmetry group where the molecular planes of ozone and water are perpendicular to the C_s symmetry plane. This structure is the same as the eclipsed structure proposed by Tachikawa and Abe [6]. Tsuge *et al.* have only compared the double-decker complex with dipole structure of Tachikawa and Abe and then predicted conflicting results. They obtained a value of 2.8661 Å for the distance between the central oxygen atoms of ozone and water, which is smaller than the experimental value (2.957 Å) [7].

This work aims to study the probable existence of O_3-H_2O complexes *via* high levels of computational chemistry in order to find the most stable structure in which the structural parameters are in good agreement with the experimental values. We have found two new configurations which have not been reported yet. All interactions in O_3-H_2O complexes are characterized by the quantum theory of atoms in molecules (QTAIM) [25-27] analysis.

COMPUTATIONAL DETAILS

The calculations were performed using the B3LYP, MP2, MP4(SDTQ), CCSD, CCSD(T), QCISD and QCISD(T) methods. The following Pople and Dunning type basis sets were used: 6-311++G(2d,2p), AUG-cc-pVDZ and AUG-cc-pVTZ. The optimizations and frequency analyses were performed using B3LYP, MP2, CCSD and QCISD methods combined with the 6-311++G(2d,2p), AUG-cc-pVDZ and AUG-cc-pVTZ (only with MP2 method) basis sets. The frequency calculations have been performed by using the default scale factor. In addition, single point calculations have been carried out with MP4(SDTQ), CCSD, CCSD(T), QCISD and QCISD(T) methods and Dunning type basis sets for the reference geometry obtained at the CCSD/AUG-cc-pVDZ level of theory. The counterpoise procedure (CP) [28] was used to correct the basis set superposition error (BSSE) in the calculation of binding energies. Geometries, energies, and frequencies were determined by using the Gaussian-03 program package [29]. The Bader's quantum theory of atoms in molecules (QTAIM) [25-27] was also applied to find critical points and to characterize them. Topological properties were calculated at MP2/6-311++G(2d,2p) level of theory by the AIM2000 program package [30].

To get a more detailed insight into the nature of weak interactions, decomposition of the interaction energy was performed by using the method proposed by Morokuma and co-workers [31]. According to this approach the total Hartree-Fock interaction energy is decomposed in the following way:

$$E(HF) = ES + EX + CT + POL + MIX$$

The term ES, the electrostatic energy term, represents the Columbic interaction energy between the charges distributions of the two subunits of the complex considered. The exchange term (EX) corresponds approximately to the steric repulsion of electron clouds. The polarization interaction energy (POL) term is connected with the internal redistribution of the electron density. The charge transfer (CT) term corresponds to the shift of electron charge between the interacting subunits. The MIX term represents the higher-order repulsive interactions. The calculations have been performed with the PC GAMESS quantum chemistry package [32].

RESULTS AND DISCUSSION

Structures **OW1-OW6** corresponds to the various ways by which H_2O can interact with O_3. Figure 1 shows the molecular graphs obtained by AIM calculations for all structures obtained in this work. Altogether, as shown in Fig. 1, we found six complexes between H_2O and O_3, of which **OW1** and **OW5** are transition states and **OW6** is a higher-order saddle point. A schematic picture of the potential energy surface of these complexes is displayed in Fig. 2. This potential curve has been obtained from the relaxed internal rotation about the O···O distance in **OW1** and O···H distance in **OW3**, **OW4**, **OW5** at B3LYP/6-311++G(2df,pd) level of theory. To the best of our knowledge, **OW5** and **OW6** have not been reported yet. Complexes **OW1-4** have the same configurations proposed by Tachikawa and Abe [2,4,6] as well as Tsuge *et al.* [24]. At all levels of theory, **OW1** and **OW2** complexes have C_s symmetry with the exception of **OW2** at QCISD(T)/AUG-cc-pVDZ and QCISD/6-311++G(2d,2p) levels, which is C_1. The oxygen of H_2O in the **OW1** and **OW2** complexes orients toward the central oxygen atom of O_3. All atoms of H_2O and the central oxygen atom of O_3 in the **OW1** are in the same plane. The symmetry plane bisects the H-O-H and O-O-O angles in the **OW2**. All atoms in the **OW3** and **OW4** complexes are located in the same plane. The H6 atom in

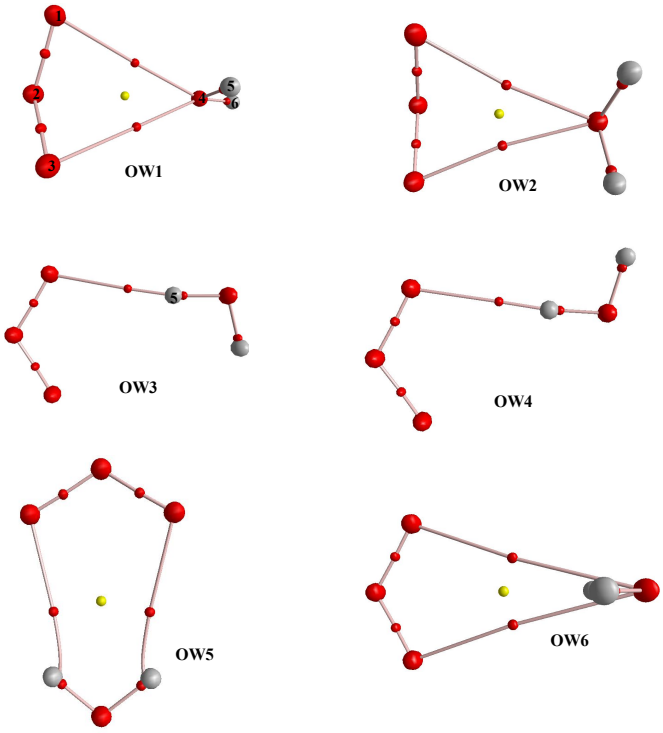

Fig. 1. Molecular graphs of O_3-H_2O complexes. Nuclei and critical points (bond and ring) are represented by big and small circles, respectively.

OW3 and **OW4** complexes is located in the direction towards O_3, and in the opposite direction towards O_3, respectively. In both structures, atom H5 of H_2O is tilted toward the terminal oxygen of O_3(O1). **OW5** and **OW6** with the planar and non-planar C_{2v} symmetry, respectively, are also hydrogen bonded complexes.

The calculated binding energies for different isomers of the O_3-H_2O complex at several levels of theory are listed in Table 1. We have computed binding energies for all isomers with reference to the isolated water and ozone molecules. As shown in Table 1, at all levels of theory, all complexes are more stable than the separated reactants H_2O and O_3. The hydrogen bonded complexes (**OW3**, **OW4** and **OW5**) as well as the non-hydrogen bonded complex **OW6** are less stable than the non-hydrogen bonded complexes **OW1** and **OW2**. All calculations indicate that the **OW2** is the most stable one**,** as predicted by Tachikawa and Abe [4,6] as well as Tsuge *et al.* [24]. The hydrogen bond interactions in **OW3**, **OW4** and **OW5** are weaker than those observed in the H_2O dimer (5.0-7.0 kcal mol^{-1}) [2]. The energies of **OW3** and **OW4** are nearly equal, in agreement with the results of Tachikawa and Abe [2].

OW1 and **OW2** complexes are non-hydrogen bonded complexes and exhibit double O···O interactions, as shown in Fig. 1. This type of interaction has been reported in some

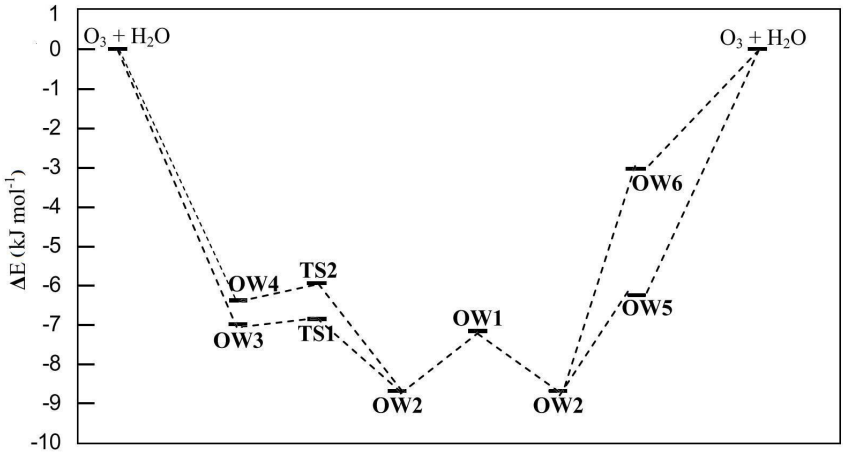

Fig. 2. Schematic diagram of the potential energy surface involving formation of the **OW1-6** complexes at B3LYP/6-311++G(2df,pd) level of theory. The structures of TS1 and TS2 are similar to the **OW3** and **OW4**, respectively.

Table 1. Calculated Binding Energies (kJ mol^{-1}) for O_3 (g) + H_2O (g) → O_3-H_2O (g)

Complex	Method	Basis set	BSSE	D_e[a]	D_e^{Bsse}	D_0	D_0^{Bsse}
OW1	B3LYP	AUG-cc-pVDZ	1.07	-5.19	-4.12	-3.05	-1.98
		AUG-cc-pVTZ	0.28	-4.71	-4.43	-2.57	-2.30
	MP2	AUG-cc-pVTZ	1.92	-11.45	-9.52	-8.23	-6.31
	CCSD	AUG-cc-pVDZ	3.54	-9.67	-6.14	-6.62	-3.09
		AUG-cc-pVTZ	1.81	-8.89	-7.08	-5.83	-4.02
	CCSD(T)	AUG-cc-pVDZ	3.91	-11.07	-7.16	-8.02	-4.11
		AUG-cc-pVTZ	1.86	-10.10	-8.24	-7.05	-5.19
	QCISD	AUG-cc-pVDZ	3.49	-9.88	-6.39	-6.83	-3.34
		AUG-cc-pVTZ	1.78	-8.52	-6.74	-5.47	-3.69
	QCISD(T)	AUG-cc-pVDZ	3.54	-10.98	-7.44	-7.93	-4.39
		AUG-cc-pVTZ	1.84	-10.12	-8.28	-7.07	-5.23
	MP4(SDTQ)	AUG-cc-pVTZ	1.95	-10.79	-8.84	-7.74	-5.79
OW2	B3LYP	AUG-cc-pVDZ	0.98	-6.57	-5.59	-2.86	-1.88
		AUG-cc-pVTZ	0.31	-6.17	-5.86	-2.46	-2.15
	MP2	AUG-cc-pVTZ	2.03	-11.84	-9.81	-8.30	-6.27
	CCSD	AUG-cc-pVDZ	2.60	-9.61	-7.01	-7.68	-5.09
		AUG-cc-pVTZ	1.77	-9.60	-7.83	-7.67	-5.90
	CCSD(T)	AUG-cc-pVDZ	3.52	-11.43	-7.91	-9.51	-5.99
		AUG-cc-pVTZ	1.58	-11.28	-9.70	-9.36	-7.78
	QCISD	AUG-cc-pVDZ	3.16	-9.85	-6.70	-7.93	-4.77
		AUG-cc-pVTZ	1.70	-9.30	-7.60	-7.37	-5.67
	QCISD(T)	AUG-cc-pVDZ	3.54	-13.74	-10.20	-11.82	-8.28
		AUG-cc-pVTZ	1.57	-10.58	-9.01	-8.66	-7.09
	MP4(SDTQ)	AUG-cc-pVTZ	2.00	-16.12	-14.12	-14.20	-12.20
OW3	B3LYP	AUG-cc-pVDZ	0.90	-6.48	-5.58	-1.86	-0.96
	MP2	AUG-cc-pVTZ	2.13	-9.80	-7.66	-5.26	-3.13
	CCSD	AUG-cc-pVDZ	3.49	-9.92	-6.42	-5.30	-1.81
OW4	B3LYP	AUG-cc-pVDZ	0.89	-5.94	-5.05	-1.48	-0.60
	MP2	AUG-cc-pVTZ	2.15	-9.26	-7.11	-5.65	-3.50
	CCSD	AUG-cc-pVDZ	2.23	-9.67	-7.44	-5.21	-2.98
OW5	B3LYP	AUG-cc-pVDZ	0.78	-4.89	-4.11	-1.48	-0.70
	MP2	AUG-cc-pVTZ	1.90	-8.59	-6.69	-4.70	-2.81
	CCSD	AUG-cc-pVDZ	2.88	-8.28	-5.40	-4.87	-1.99
OW6	B3LYP	AUG-cc-pVDZ	0.47	-2.05	-1.58	-0.39	0.08
	MP2	AUG-cc-pVTZ	1.02	-4.31	-3.29	-2.44	-1.42
	CCSD	AUG-cc-pVDZ	1.90	-4.85	-2.95	-3.19	-1.30

D_e^{BSSE} = Electronic binding energy (D_e) + BSSE, $D_0 = D_e + \Delta ZPE$, $D_0^{BSSE} = D_0 + BSSE$.

complexes such as O_3-H_2O_2 [33] and O_3-HOCl complexes [19]. After inclusion of both ZPVE and BSSE corrections, the binding energies of **OW1** and **OW2**, by using the CCSD/AUG-cc-pVDZ geometry, emerge in -5.79 and -12.20 kJ mol^{-1} at MP4/AUG-cc-pVTZ, -4.11 and -5.99 kJ mol^{-1} at CCSD(T)/AUG-cc-pVDZ, -5.19 and -7.78 kJ mol^{-1} at CCSD(T)/AUG-cc-pVTZ, -4.39 and -8.28 kJ mol^{-1} at QCISD(T)/AUG-cc-pVDZ and -5.23 and -7.09 kJ mol^{-1} at QCISD(T)/AUG-cc-pVTZ levels, respectively. ZPVE and BSSE corrected binding energies of **OW1** and **OW2** at the

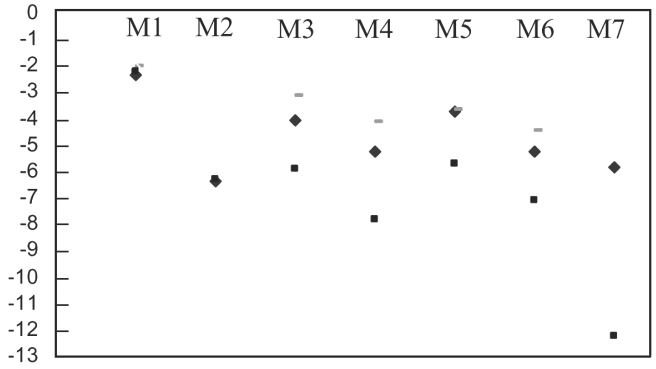

Fig. 3. Schematic representation of the relative energies of **OW1** and **OW2** at the various level of theory. M1 = B3LYP, M2 = MP2, M3 = CCSD, M4 = CCSD(T), M5 = QCISD, M6 = QCISD(T) and M7 = MP4(SDTQ): (◆) **OW1**(AUG-cc-pVTZ); (—) **OW1**(AUG-cc-pVDZ); (■) **OW2**(AUG-cc-pVTZ) and (×) **OW2**(AUG-cc-pVDZ).

various levels of theory are also shown in Fig. 3. This figure shows that the highest and lowest values of binding energies correspond to the MP4(SDTQ) and B3LYP methods, respectively. After the MP4(SDTQ) method, CCSD(T) method in conjunction with the AUG-cc-pVTZ basis set predicts the binding energy of -7.8 kJ mol^{-1} for the most stable complex **OW2**. As seen in Fig. 3, the energy difference obtained using AUG-cc-pVDZ and AUG-cc-pVTZ basis sets for **OW2** is the smallest for the B3LYP method and the greatest for the CCSD(T) one.

The complexes **OW3-OW6** were optimized at B3LYP/AUG-cc-pVDZ, CCSD/AUG-cc-pVDZ, QCISD/6-311++G(2d,2p) and MP2/AUG-cc-pVTZ levels. **OW1** and **OW2** were selected and reoptimized at QCISD/AUG-cc-pVDZ, QCISD(T)/AUG-cc-pVDZ and CCSD(T)/AUG-cc-pVDZ levels of theory. The complex **OW1** is not stable at QCISD(T)/AUG-cc-pVDZ and CCSD(T)/AUG-cc-pVDZ levels and is converted to **OW2** complex during the optimization. Table 2 presents geometrical parameters of the O_3-H_2O complexes. Inspection of Table 2 reveals that the interaction between O_3 and H_2O results in a small change of geometry of H_2O. The **OW2** complex has C_s symmetry at MP2/AUG-cc-pVTZ, QCISD/AUG-cc-pVDZ and CCSD/AUG-cc-pVDZ levels and C_1 symmetry at QCISD(T)/AUG-cc-pVDZ and QCISD/6-311++G(2d,2p) levels of theory. The O4-H5 distance is elongated by 0.001 Å upon complex formation of **OW2** at CCSD/AUG-cc-pVDZ and MP2/AUG-cc-pVTZ levels while there is no change in it at QCISD/AUG-cc-pVDZ and QCISD(T)/AUG-cc-pVDZ levels. Both O-O bonds of O_3 in **OW2** are shortened by 0.001 Å at CCSD/AUG-cc-pVDZ and MP2/AUG-cc-pVTZ levels.

Decrease in O1-O2 and O2-O3 bond lengths of O_3 at QCISD(T)/AUG-cc-pVDZ level is 0.003 and 0.001 Å, respectively. The O-O bond lengths of O_3 at QCISD/AUG-cc-pVDZ level are decreased upon complexation by 0.002 Å. Changes in the H5-O4-H6 angle of H_2O and O1-O2-O3 angle of ozone upon complexation are very small. The calculated distance between the center of mass of O_3 and H_2O (O2···O4) is 2.932, 2.927, 2.934, 3.093 and 3.111 Å at MP2/AUG-cc-pVTZ, QCISD(T)/AUG-cc-pVDZ, QCISD/6-311++G(2d,2p), CCSD/AUG-cc-pVDZ and QCISD/AUG-cc-pVDZ levels of theory, respectively. The values obtained at MP2/AUG-cc-pVTZ, QCISD/6-311++G(2d,2p) and QCISD(T)/AUG-cc-pVDZ levels are in close agreement with the experimental value of 2.957 Å. The percentage error in our calculated O2···O4 distance is smaller than 1.0%. The O2···O4 distance reported by Tachikawa and Abe [6] and Tsuge *et al.* [24] at QCISD/6-311++G(d,p) level is 2.8587 and 2.8613 Å, respectively. Thus, in comparison with the reported O2···O4 distance [6,24], the values obtained in this work are closer to the experimental one. The O1-O2(O2-O3), O4-H5 and O2···O4 distances in complex **OW1** are 1.284, 0.962 and 2.947 Å at MP2/AUG-cc-pVTZ level of theory. The O2···O4 distances in complex **OW2** are smaller than those of complex **OW1**.

The change in the IR spectra originated by the formation of the complexes is a useful tool to identify experimentally complexes. Table 3 shows the not scaled vibrational

Table 2. Optimized Geometrical Parameters (Å and °) for Monomers (Given in Parentheses) and Complexes at Different Levels of Theory

Parameter	**OW1**				**OW2**				
	L1	*L2*	*L3*	*L4*	*L1*	*L2*	*L3*	*L4*	*L5*
O1-O2	1.284	1.259	1.263	1.259	1.283 (1.284)	1.258 (1.259)	1.262	1.258	1.284
O2-O3	1.284	1.259	1.263	1.259	1.283	1.258	1.262	1.259	1.286
O4-H5	0.962	0.965	0.965	0.957	0.962 (0.961)	0.965 (0.964)	0.965 (0.965)	0.957	0.967 (0.967)
O4-H6	0.961	0.964	0.964	0.956	0.962	0.965	0.965	0.957	0.967
O1···O4	2.890	3.006	3.008	3.050	2.921	3.062	3.062	3.158	3.280
O2···O4	2.947	3.109	3.114	2.997	2.932	3.093	3.111	2.934	2.927
O3···O4	2.890	3.005	3.008	3.050	2.921	3.062	3.062	3.130	3.039
O1-O2-O3	116.5	117.1	117.2	117.8	116.5 (116.7)	117.2 (117.3)	117.3 (117.4)	117.8	116.7 (117.4)
H5-O4-H6	104.5	104.5	104.5	104.8	104.1 (104.1)	103.9 (104.2)	103.8 (104.1)	104.6	103.9 (103.9)

	OW3			**OW4**		**OW5**		**OW6**		
	L1	*L2*	*L4*	*L1*	*L2*	*L4*	*L1(L4)*	*L2*	*L1(L4)*	*L2*
O1-O2	1.281	1.260	1.265	1.281	1.263	1.273	1.284(1.260)	1.259	1.284(1.261)	1.259
O2-O3	1.287	1.260	1.256	1.287	1.256	1.249	1.284(1.260)	1.259	1.284(1.261)	1.259
O4-H5	0.963	0.965	0.957	0.963	0.965	0.958	0.962(0.957)	0.964	0.961(0.956)	0.964
O4-H6	0.961	0.964	0.956	0.961	0.964	0.956	0.962(0.957)	0.964	0.961(0.956)	0.964
O1···H5	2.365	2.305	2.274	2.365	2.387	2.276	2.535(2.655)	2.535	-	-
O3···H5	2.583	2.671	2.873	2.583	2.523	2.847	-	-	-	-
O1-O2-O3	116.3	117.0	117.7	116.3	116.9	117.7	116.8(117.9)	117.3	116.5(117.7)	117.1
H5-O4-O6	104.2	104.2	104.4	104.2	104.2	104.6	102.7(103.4)	102.7	103.0(103.6)	103.2

L1 = MP2/AUG-cc-pVTZ. *L2* = CCSD/AUG-cc-pVDZ. *L3* = QCISD/AUG-cc-pVDZ. *L4* = QCISD/6-311++G(2d,2p). *L5* = QCISD(T)/AUG-cc-pVDZ.

frequencies for O_3, H_2O and complexes **OW1-6**. Formation of O_3-H_2O complex from two nonlinear molecules converts three degrees of rotational and three degrees of translational freedom into six new low-frequency intermolecular modes which lie bellow 400 cm^{-1}. Table 3 evidently shows that the **OW1, OW5** and **OW6** complexes are saddle points. **OW1** and **OW5** are transition states and **OW6** is higher-order saddle point. The relax potential scan for the internal rotation about the O···O distance, at B3LYP/6-311++G(2df,pd) level, reveals that the **OW1** is a transition state between two **OW2** structures, as shown in Fig. 2. Although, the QCISD, CCSD and QCISD(T) methods using Dunning type basis set (AUG-cc-pVDZ) give good geometries for O_3-H_2O complex, they provide poor intermolecular vibrational modes. Accordingly, one imaginary frequency corresponds to intermolecular vibrational mode was found for **OW2** at the CCSD/AUG-cc-pVDZ (-74.0 cm^{-1}), MP2/AUG-cc-pVTZ (-65.2 cm^{-1}), QCISD/AUG-cc-pVDZ (-84.8 cm^{-1}) and QCISD(T)/AUG-cc-pVDZ (-50.1 cm^{-1}) levels. The experimental study [24] shows that the O_3-H_2O complex has eclipsed (**OW2**) configuration. All the vibrational frequencies of **OW2** at the QCISD/6-311++G(d,p) [24], QCISD/6-311++G(2d,2p) and CCSD(T)/6-311++G(d,p) [24] levels are real numbers. At local minimum, all the vibrational frequencies are real numbers. Thus, the vibrational frequencies obtained by using QCISD and CCSD(T) methods in conjunction with Pople basis sets should be more reliable. Besides, the QCISD method in conjunction with 6-311++G(d,p) (no reported) and 6-311++G(2d,2p) basis sets (Table 3) predict positive vibrational frequencies for *cis* (**OW3**) and *trans* (**OW4**) complexes. In addition, B3LYP

Table 3. Harmonic Vibrational Frequencies (cm^{-1}) Calculated at QCISD/6-311++G(2d,2p) Level of Theory. Experimental Values [24] are Given in Parentheses

	Mode	Monomer	**OW1**	**OW2**	**OW3**	**OW4**	**OW5**	**OW6**
H_2O								
	ν_3[b]	3984.0 (3750.7)	3979.7	3977.8	3975.8	3974.6	3975.0	3980.8
	ν_1[a]	3881.8 (3660.7)	3876.8	3876.5	3878.1	3875.0	3884.3	3885.1
	ν_2[c]	1686.1 (1595.6)	1686.3	1688.1 (1598.3	1694.7	1695.1	1695.5	1690.2
O_3								
	ν_1[a]	1229.6 (1104.3)	1234.9	1237.6 (1110.0)	1234.7	1250.4	1231.6	1229.7
	ν_3[b]	931.2 (1039.9)	932.4	941.6 (1045.3)	919.5	896.9	924.6	926.4
	ν_2[c]	736.3 (699.5)	740.8	740.6 (703.4)	742.2	737.0	738.7	740.1
	Int.[d]							
	ν_1		158.4	158.4	345.3	354.3	275.2	146.3
	ν_2		100.1	126.9	169.8	181.6	122.0	65.5
	ν_3		78.0	100.0	99.2	93.1	74.1	58.6
	ν_4		37.4	73.5	97.3	78.8	66.7	12.7
	ν_5		13.9	61.2	40.6	42.2	33.4	i119.5
	ν_6		i74.1	34.3	30.4	38.8	i137.6	i143.6

[a]Symmetric stretching. [b]Asymmetric stretching. [c]Bending. [d]Intermolecular.

method combined with the 6-311++G(2d,2p), AUG-cc-pVDZ and AUG-cc-pVTZ basis sets (no reported) give positive vibrational frequencies for the *cis* (**OW3**) and *trans* (**OW4**) complexes. The DFT methods predict vibrational frequencies of the ozone very well, yielding results comparable to those at the CCSD or CCSD(T) levels [34]. As a result, in agreement with Tachikawa and Abe's results [2] and in disagreement with Tsuge *et al.*'s conclusion [24], they could not be transition states connecting two eclipsed (**OW2**) forms. They are true minima on the potential energy surface.

The calculated harmonic vibrational frequencies, reported in Table 3, at QCISD/6-311++G(2d,2p) level, for **OW2** are in good agreement with the observed frequencies [24]. It is worth noting that the higher three intermolecular modes belong to the H_2O moiety. All the vibrational frequencies of H_2O in **OW2** are slightly changed upon complexation, in agreement with the small changes of structural parameters and small complexation energies. In **OW2**, the OH stretching modes are red-shifted whereas the H-O-H bending mode is blue-shifted. All of the vibrational frequencies of O_3 are weakly blue-shifted upon complex formation. The shifts in the vibrational frequencies are significantly low, indicating that the interaction between water and ozone is very week. As seen in Table 3, directions of the frequency shift calculated at QCISD/6-311++G(2d,2p) level for **OW2** are in good agreement with observed ones.

Rotational constants for the complexes and monomers were calculated at several levels. Three experimentally different values of the rotational constants (A = 11.9606, B = 4.1740 and 3.2652 GHz) for complex O_3-H_2O indicate that this is an asymmetric rotor. The calculated rotational constants for **OW2** at the QCISD/AUG-cc-pVDZ and CCSD/AUG-cc-pVDZ levels are A = 11.7731, 11.8349, B = 4.331, 4.3323 and C = 3.3584, 3.3692 GHz, respectively. The consistency between calculated and experimental rotational constant values for **OW2** is quite well. Thus, it is predicted that **OW2**

is a suitable candidate for the structure of the O_3-H_2O complex observed experimentally in the gas phase.

The computed dipole moments for complex **OW2** at QCISD/AUG-cc-pVDZ, CCSD/AUG-cc-pVDZ and QCISD/AUG-cc-pVDZ levels of theory are 1.32, 1.28, 1.29 D, in agreement with experimental value of 1.14 D.

OW1 and **OW2** were investigated using the interaction energy decomposition proposed by Morokuma and co-workers. The results are given in Table 4. The results of energy decomposition for **OW3-6** are not included in Table 4 due to the difficulties connected with the convergence of the decomposition within the Morokuma scheme. The ES, EX, POL and CT terms were described in the computational method section. It is well known that the electrostatic term plays the most important role for hydrogen bond interactions [35-37]. According to the ES term, the electrostatic character of interaction is more significant for **OW2** than that for **OW1**. The EX term and higher-order attractive terms (POL and CT) are also greater in **OW2** than those for **OW1**. For **OW1**, the electrostatic and the exchange energy terms are approximately equal. For **OW2**, exchange term outweighs the electrostatic terms. The greater stability of **OW2** might be attributed to the greater higher-order attractive terms observed in **OW2** compared with **OW1**.

The quantum theory of atoms in molecules (QTAIM) is a useful tool to characterize weak hydrogen bonding [38-42]. The values of electron density, ρ(r), Laplacian of electron density, $\nabla^2\rho(r)$, electronic energy density, H(r), electronic kinetic energy density, G(r), and electronic potential energy density, V(r), at bond critical points (BCPs), calculated at the MP2/6-311++G(2d,2p) level of theory, are listed in Table 5. The presence of the intermolecular bond critical points is an indication of interaction between the species involved. As shown in Fig. 1, there are two BCPs and one ring critical point (RCP), in the region between the H_2O and O_3, for non-hydrogen bonded complexes **OW1** and **OW2**. The values of ρ(r) and $\nabla^2\rho(r)$ are in the range of weak interactions. Comapring the BCP data ($\nabla^2\rho(r) > 0$ and $H(r) > 0$) give us the confidence that the O···O interactions are electrostatic in character. The values of ρ(r) and $\nabla^2\rho(r)$, at O···O BCPs, in the most stable complex **OW2** are greater than those for **OW1**. The RCP data observed in **OW2** are also greater than in **OW1**. Thus, strong interactions correspond to the most stable complex.

Table 4. Interaction Energy (kJ mol^{-1}) Components of most Stable Complexes According to Morokuma Scheme

Energy component	**OW1**	**OW2**
ES	-8.74	-14.80
EX	8.65	16.72
PL	-1.25	-3.05
CT	-1.59	-2.51
MIX	0.59	2.13
ΔE_{SCF}	-2.30	-1.55

The comparison of BCP data of O-O bonds in the complexes **OW1** and **OW2** with the O_3 monomer shows that ρ(r) increases slightly upon complexation, in agreement with the small decrease of the O-O bond distance as well as the weak blue shift of the corresponding vibrational frequency. The negative signs of $\nabla^2\rho(r)$ and H(r) at O-O and O-H BCPs show that these bonds are covalent in nature, indicating the concentration of electronic charge between the nuclei. The covalent character of the O-O bonds increases and that of O-H bonds decreases upon complexation, because the corresponding $\nabla^2\rho(r)$ as well as H(r) values increase and decrease, respectively. Changes in BCP data for complex formation of **OW2** are greater than those for **OW1**.

In complexes **OW3** and **OW4**, there is one BCP in O1···H5 distance, indicating interaction between H_2O and O_3 through hydrogen bonding. The values of ρ(r) and $\nabla^2\rho(r)$ at the O1···H5 BCP of both complexes are in the typical range of ρ(r) (0.002-0.035 a.u.) and $\nabla^2\rho(r)$ (0.020-0.139 a.u.) for H-bonding [41]. The small electron density and positive values of $\nabla^2\rho(r)$ as well as H(r) at the O···H5 BCPs are typical for closed-shell interaction with charge depletion between the nuclei. They are electrostatic in nature. The values of ρ(r) and $\nabla^2\rho(r)$ in **OW3** are the greater than those in **OW4**, in agreement with greater binding energy calculated for **OW3** compared with **OW4**.

The comparison of QTAIM data of the O4-H5 bond of complexes **OW3** and **OW4** with H_2O monomer shows that the ρ(r) decreases upon H-bonding, in agreement with the increase of its bond distance as well as the red shift of its corresponding vibrational frequency. $\nabla^2\rho(r)$ and H(r) values for O4-H5 bonds

Table 5. Bond Critical Point Data (a.u.) Calculated at MP2/6-311++G(2d,2p) Level of Theory

	ρ(r)	$\nabla^2\rho(r)$	G(r)	V(r)	H(r)	ρ(r)	$\nabla^2\rho(r)$	G(r)	V(r)	H(r)
			O_3					**H_2O**		
O1-O2	0.4224	-0.1249	0.3763	-0.7838	-0.4075					
O2-O3	0.4224	-0.1249	0.3763	-0.7838	-0.4075					
O4-H5						0.3791	-2.9202	0.0719	-0.8738	-0.8019
O4-H6						0.3791	-2.9202	0.0719	-0.8738	-0.8019
			OW1					**OW2**		
O1-O2	0.4227	-0.1287	0.3755	-0.7831	-0.4076	0.4235	-0.1331	0.3753	-0.7838	-0.4085
O2-O3	0.4227	-0.1287	0.3755	-0.7831	-0.4076	0.4235	-0.1331	0.3753	-0.7838	-0.4085
O1···O4	0.0079	0.0338	0.0074	-0.0064	0.0010	0.0088	0.0350	0.0079	-0.0070	0.0009
O4-H6	0.3789	-2.9192	0.0718	-0.8734	-0.8016	0.3781	-2.9144	0.0714	-0.8714	-0.8000
O4-H5	0.3775	-2.9158	0.0708	-0.8705	-0.7997	0.3781	-2.9144	0.0714	-0.8714	-0.8000
O3···O4	0.0079	0.0338	0.0074	-0.0064	0.0010	0.0088	0.0350	0.0079	-0.0070	0.0009
RCP	0.0070	0.0364	0.0077	-0.0064	0.0013	0.0084	0.0391	0.0085	-0.0073	0.0012
			OW3					**OW4**		
O1-O2	0.4235	-0.1309	0.3768	-0.7862	-0.4094	0.4260	-0.1417	0.3785	-0.7924	-0.4139
O3-O2	0.4215	-0.1214	0.3754	-0.7812	-0.4058	0.4188	-0.1100	0.3734	-0.7742	-0.4008
O1···H5	0.0110	0.0469	0.0099	-0.0081	0.0018	0.0103	0.0434	0.0092	-0.0075	0.0017
O4-H5	0.3763	-2.9282	0.0697	-0.8714	-0.8017	0.3761	-2.9277	0.0695	-0.8710	-0.8015
O4-H6	0.3791	-2.9092	0.0726	-0.8726	-0.7999	0.3793	-2.9085	0.0728	-0.8727	-0.7999
			OW5					**OW6**		
O1-O2	0.4284	-0.1460	0.3813	-0.7990	-0.4178	0.4224	-0.1247	0.3764	-0.7839	-0.4075
O2-O3	0.4284	-0.1460	0.3813	-0.7990	-0.4178	0.4224	-0.1247	0.3764	-0.7839	-0.4075
O1···H4(O4)	0.0069	0.0268	0.0058	-0.0050	0.0009	0.0029	0.0132	0.0026	-0.0019	0.0007
O4-H6	0.3753	-2.8847	0.0707	-0.8626	-0.7919	0.3789	-2.9190	0.0719	-0.8735	-0.8016
O4-H5	0.3753	-2.8847	0.0707	-0.8626	-0.7919	0.3789	-2.9190	0.0719	-0.8735	-0.8016
O3···H5(O4)	0.0069	0.0268	0.0058	-0.0050	0.0009	0.0029	0.0132	0.0026	-0.0019	0.0007
RCP	0.0044	0.0205	0.0042	-0.0033	0.0009	0.0025	0.0126	0.0024	-0.0016	0.0008

Table 6. Atomic Charges (CHelpG) for the Complexes **OW1-OW4** at MP2/6-311++G(2d,2p) Level

CHelpG charge (a.u.)	**O_3**	**H_2O**	**OW1**	**OW2**	**OW3**	**OW4**
O1	-0.1418		-0.1454	-0.1526	-0.1032	-0.1409
O2	0.2835		0.2862	0.2894	0.2637	0.2568
O3	-0.1418		-0.1454	-0.1526	-0.1279	-0.0817
O4		-0.7488	-0.7291	-0.7014	-0.7521	-0.7705
H5		0.3744	0.3561	0.3586	0.3477	0.3511
H6		0.3744	0.3776	0.3586	0.3718	0.3852
Charge transfer			*-0.0046*	*-0.0158*	*0.0326*	*0.0342*

involved in hydrogen bonding are negative, indicating the covalent nature of these bonds. The H(r) values of O4-H5 bonds predict that the covalent nature of the bond in both complexes decreases upon complexation, since the corresponding H(r) in these complexes is lesser negative than that of H_2O monomer.

Analysis of the BCP data in **OW5** and **OW6** shows that O···H and O···O interactions are electrostatic in nature. Topological parameters of O···H interactions in **OW5** are smaller than those for **OW3** and **OW4**, indicating that hydrogen bond interaction in **OW5** is weaker than that for **OW3** and **OW4**. A comparison of topological parameters of O···O interactions in **OW6**, **OW1** and **OW2** reveals that this interaction in **OW6** is weaker than that in **OW1** and **OW2**.

CHelpG [43] (Charges from Electrostatic Potentials using a Grid based method) charge analysis for the complexes **OW1**-**OW4** and monomers are given in Table 6. The charge transfer can be defined as the sum of atomic charges on the O_3 moiety in the complexes. In the non-hydrogen bonded complexes **OW1** and **OW2**, the results show that the O1 and O3 atoms of ozone gain, and the O2 atom loses, electronic charge, resulting in a charge transfer of 0.0046 and 0.0158 a.u. from H_2O to O_3 in **OW1** and **OW2**, respectively. The amounts of charge transfer in the non-hydrogen bond complexes are correlated to the complexation energies. In contrast, the O1 and O3 atoms of ozone involved in the hydrogen bonded complexes **OW3** and **OW4** lose electronic charge upon complexation, which means that overall charge transfer take places from the O_3 moiety to the H_2O.

CONCLUSIONS

Quantum chemical calculations have been carried out for the O_3-H_2O complexes in order to examine their structural characteristics and energetics at high levels of theory. We found six complexes. Three of them are in local minimum. Two different intermolecular interactions were expected to participate in the formation of complexes, namely conventional O···H hydrogen bonding and O···O interaction. Three of the complexes found are non-hydrogen bonded and exhibit the double O···O interactions whereas the remaining complexes are hydrogen bonded. The binding energies of the most stable complex corrected with BSSE and ZPE range from -5.99 to -12.20 kJ mol^{-1} at CCSD(T)/AUG-cc-pVTZ, QCISD(T)/AUG-cc-pVTZ and MP4(SDTQ)/AUG-cc-pVTZ high levels of theory. The calculated equilibrium distance between centers of the monomers (O_3···OH_2) in the most stable complex at QCISD(T)/AUG-cc-pVDZ and QCISD/6-311++G(2d,2p) levels is in good agreement with the experimental value. Bader's quantum theory of atoms in molecules (QTAIM) has been employed to elucidate the interaction characteristics of the O_3-H_2O complexes. The AIM calculations predict that the O···O and O···H interactions in O_3-H_2O complexes are electrostatic in nature.

REFERENCES

[1] R.P. Wayne, Chemistry of Atmospheres, Claredon Press, Oxford, 1991.

[2] H. Tachikawa, S. Abe, Inorg. Chem. 42 (2003) 2188.

[3] Y. Bedjanian, G. Poulet, Chem. Rev. 103 (2003) 4639.

[4] H. Tachikawa, S. Abe, Inorg. Chim. Acta 358 (2005) 288.

[5] H. Roohi, B. Mackiabadi, Bull. Chem. Soc. Jpn. 80 (2007) 1914.

[6] H. Tachikawa, S. Abe, Chem. Phys. Lett. 432 (2006) 409.

[7] J.Z. Gillies, C.W. Gillies, R.D. Suenram, F.J. Lovas, T. Schmidit, D. Cremer, J. Mol. Spectrosc. 146 (1991) 493.

[8] L. Schriver, C. Barreau, A. Schriver, Chem. Phys. 140 (1990) 429.

[9] A. Engdahl, B. Nelander, Chem. Phys. 293 (2003) 203.

[10] Z. Mielka, L. Andrews, J. Phys. Chem. 94 (1990) 3519.

[11] L. Andrews, R. Withnall, R.D. Hunt, J. Phys. Chem. 92 (1988) 78.

[12] H. Tachikawa, S. Abe, T. Iyama, Inorg. Chem. 40 (2001) 1167.

[13] R. Withnall, R.M. Hawkins, M.L. Andrews, J. Phys. Chem. 90 (1985) 575.

[14] A.J.C. Varandas, L. Zhang, Chem. Phys. Lett. 385 (2004) 409.

[15] M. Venayagamoorthy, T.A. Ford, J. Mol. Struct. 651 (2003) 223.

[16] L. Andrews, R. Withnall, B.W. Moors, J. Phys. Chem. 93 (1989) 1279.

[17] C. Lugez, A. Schriver, R. Levant, L. Schriver-Mazzuoli, Chem. Phys. 181 (1994) 129.

[18] B. Makiabadi, H. Roohi, Chem. Phys. Lett. 460 (2008)

72.

[19] M. Solimannejad, I. Alkotra, J. Elguero, Chem. Phys. Lett. 449 (2007) 23.

[20] Y. Sadanaga, A. Yoshino, S. Kato, Y. Kajii, Environ. Sci. Technol. 39 (2005) 8847.

[21] B.J. Finlayson-Pitts, J.C. Hemminger, J. Phys. Chem. A 104 (2000) 11463.

[22] G. Frost, V.J. Vaida, Geophys. Res. Atm. 100 (1995) 18803.

[23] V. Vaida, G. Frost, L.A. Brown, R. Naaman, Y. Hurwitz, Ber. Bunsen. Phys. Chem. 99 (1995) 371.

[24] M. Tsuge, K. Tsuji, A. Kawai, A. Kawai, K. Shibuya, J. Phys. Chem. A 111 (2007) 3540.

[25] R.F.W. Bader, Atoms In Molecules, A Quantum Theory, Clarendon Press, Oxford, UK, 1990.

[26] R.F.W. Bader, H. Essen, J. Chem. Phys. 80 (1994) 1943.

[27] R.F.W. Bader, Can. J. Chem. 76 (1998) 973.

[28] S.F. Boys, F. Bernardi, Mol. Phys. 19 (1990) 553.

[29] M.J. Frisch, G.W. Trucks, H.B. Schlegel, G.E. Scuseria, M.A. Robb, J.R. Cheeseman, J.A. Montgomery Jr., T. Vreven, K.N. Kudin, J.C. Burant, J.M. Millam, S.S. Iyengar, J. Tomasi, V. Barone, B. Mennucci, M. Cossi, G. Scalmani, N. Rega, G.A. Petersson, H. Nakatsuji, M. Hada, M. Ehara, K. Toyota, R. Fukuda, J. Hasegawa, M. Ishida, T. Nakajima, Y. Honda, O. Kitao, H. Nakai, M. Klene, X. Li, J.E. Knox, H.P. Hratchian, J.B. Cross, C. Adamo, J. Jaramillo, R. Gomperts, R.E. Stratmann, O. Yazyev, A.J. Austin, R. Cammi, C. Pomelli, J.W. Ochterski, P.Y. Ayala, K. Morokuma, G.A. Voth, P. Salvador, J.J. Dannenberg, V.G. Zakrzewski, S. Dapprich, A.D. Daniels, M.C. Strain, O. Farkas, D.K. Malick, A.D. Rabuck, K. Raghavachari, J.B. Foresman, J.V. Ortiz, Q. Cui, A.G. Baboul, S. Clifford, J. Cioslowski, B.B. Stefanov, G. Liu, A. Liashenko, P. Piskorz, I. Komaromi, R.L. Martin, D.J. Fox, T. Keith, M.A. Al-Laham, C.Y. Peng, A. Nanayakkara, M. Challacombe, P.M.W. Gill, B. Johnson, W. Chen, M.W. Wong, C. Gonzalez, J.A. Pople, GAUSSIAN 03, Revision B.05, Gaussian, Inc., Pittsburgh PA, 2003.

[30] F. Biegler-König, J. Schönbohm, D. Bayles, AIM2000-A Program to Analyze and Visualize Atoms in Molecules, J. Comp. Chem. 22 (2001) 545.

[31] K. Kitaura, K. Morokuma, Int. J. Quantum Chem. 10 (1976) 325.

[32] A.A. Granovsky, PC GAMESS version 7.1, http://classic.chem.msu.su/gran/gamess/index.html.

[33] B. Makiabadi, H. Roohi, Chem. Phys. Lett. 460 (2008) 72.

[34] F. Jensen, Introduction to Computational Chemistry, John Wiley & Sons, New York, 1999.

[35] S. Scheiner, Hydrogen Bonding, A Theoretical Perspective, Oxford University Press, New York, 1997.

[36] S.J. Grabowski, W.A. Sokalski, J. Leszczynski, J. Phys. Chem. 108 (2004) 1806.

[37] S.J. Grabowski, Hydrogen Bonding-New Insights, Springer, 2006.

[38] M.T. Carroll, C. Chang, R.F.W. Bader, Mol. Phys. 63 (1988) 387.

[39] M.T. Carroll, R.F.W. Bader, Mol. Phys. 65 (1988) 695.

[40] S. Vijayakumar, P. Kolandaivel, J. Mol. Struc. 734 (2005) 157.

[41] U. Koch, P.L.A. Popelier, J. Phys. Chem. 99 (1995) 9747.

[42] P.L.A. Popelier, J. Phys. Chem. A 102 (1998) 1873.

[43] C.M. Breneman, K.B. Wiberg, J. Comput. Chem. 11 (1990) 361.